CWE-8
June 7-11, 2026
London, ON, Canada

Topographic effects on near-surface winds over an actual hilly island using CFD simulations

Shengming Tang [a], Nuohao Zhang [a,b]

[a]*Shanghai Typhoon Institute of China Meteorological Administration, Shanghai, China, tangsm@typhoon.org.cn*
[b]*State Key Laboratory of Subtropical Building and Urban Science, South China University of Technology, Guangzhou, Guangdong Province, China, nuohaozhang2000@163.com*

SUMMARY

This study employs computational fluid dynamics (CFD) to numerically investigate the influence of local topographic relief on the three-dimensional near-surface wind field over a coastal hilly island in China. A novel method employing the ERA5 reanalysis data as the background wind field to match the CFD inlet demonstrated satisfactory performance of the simulated wind field, with low root-mean-square errors for wind speed (0.40 m/s) and wind direction (16.31°). The results indicate that the wind speed acceleration and deceleration are more pronounced near the surface than at upper levels, and the vertical range influenced by the actual hilly terrain far exceeds that considered in current building load codes. At a given horizontal slope length, the horizontal wind speed ratio first increases and then decreases after reaching a critical slope angle. The current load codes are suggested to be optimized for areas with steep slopes and gentle downhill slopes.

Keywords: *CFD, wind field, slope angle, slope length, hilly terrain*

1. INTRODUCTION

Airflow over hilly terrain involves complex flow phenomena such as topographic speed-up, flow separation, and reattachment due to topographical disturbances. Understanding near-surface wind characteristics in hilly areas is critical for various applications, such as improving numerical prediction models, optimizing wind farm layouts, monitoring air pollutant dispersion, and estimating wind loads on structures.

The computational fluid dynamics (CFD) method has proven effective in simulating fine wind fields at microscales (<1 km) over hilly terrain. At present, there are two methods that are most commonly used in CFD: the large eddy simulation (LES) method and the Reynolds-averaged Navier–Stokes (RANS) method. Many studies have utilized the RANS method to simulate near-surface wind fields over actual hilly terrains. For example, Moreira et al. (2012) evaluated the performance of various RANS equations in modeling wind flow over Askervein Hill in Scotland. Blocken et al. (2015) conducted an evaluation of RANS simulations using a revised k–ε model to assess wind speed patterns over the natural complex terrain of Ria de Ferrol, Galicia, Spain. The simulated results of Blocken et al. (2015) were compared with the wind speed ratio and wind direction recorded by ultrasonic anemometers, even though comparisons with the actual wind velocity were not included because of the unknown ambient wind conditions. Jubayer and Hangan (2018) applied both the CFD method and wind tunnel tests to predict the wind flow on an actual mountain ridge in British Columbia, Canada. The results of Jubayer and Hangan (2018) showed that the speed-up factors recommended by the National Building Code of Canada (NBCC, 2015, 2016) overestimated the speed-up effect over complex configurations. The above two studies

primarily focused on the wind speed-up effect under current guidelines. However, systematic studies of the impact of local topography on wind characteristics over actual hilly terrains remains limited.

A review of historical studies on wind characteristics over actual hilly terrain indicates that the influences of local topographic relief on near-surface wind characteristics over actual hilly terrain remain unclear. In this study, the impact of topography on the near-surface wind characteristics over a specified hilly island in China is numerically investigated using CFD simulations; these simulations are then verified using a novel method that combines field measurement data and reanalysis data.

2. METHODS

The study case is Nan'ao Island in Guangdong Province, China. Nan'ao Island is a bedrock continental island consisting of east and west parts that is located between 116° 56' E and 117° 9' E longitude and 23° 24' N and 23° 29' N latitude, covering a total area of approximately 117.73 km^2. The island consists of irregular hilly terrain with peak altitudes of approximately 573 m in the east and 588 m in the west. A schematic diagram of the study area is illustrated in Figure 1.

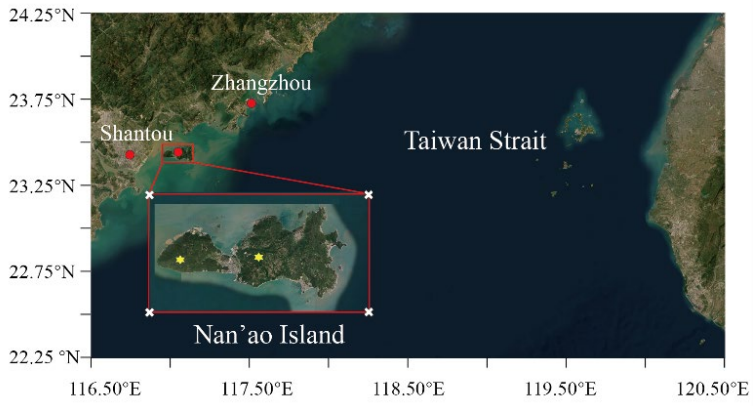

Figure 1. Schematic diagram of the study area (Nan'ao Island) of the CFD simulation.

The numerical simulations were performed with the commercial CFD code ANSYS/Fluent, employing the control volume method to solve the three-dimensional (3D) steady RANS equations. The realizable k–ε model was adopted to provide closure. Third-order monotonic upstream-centered scheme for conservation laws (MUSCL) discretization schemes were used for both the convective and viscous terms of the governing equations. The SIMPLEC algorithm was used for the pressure–velocity coupling, and a pressure staggered option (PRESTO) was specified for the pressure interpolation. Calculations were performed for 16 wind directions with an interval of 22.5°. Convergence was assumed to be obtained when all the scaled residuals had levelled off and were less than 5×10^{-4}. In this study, the computational domain is scaled with a ratio of 1:300, which is consistent with the geometric scale ratio in a wind tunnel test (Fang et al., 2009). The length, width, and height of the computational model are 1500 m, 700 m, and 35 m, respectively. The horizontal grid spacing in the densified region of Nan'ao Island is 0.33 m, and the resulting total grid contains approximately 4 million control volumes (Figure 2).

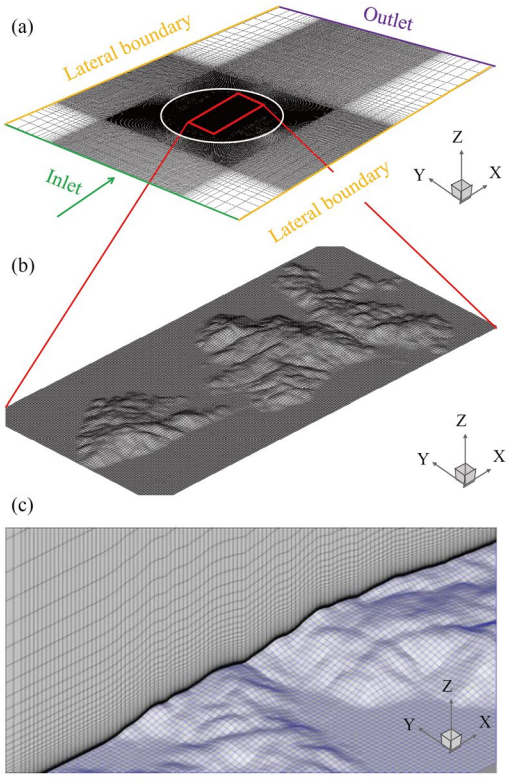

Figure 2. Computational grid in the CFD model. (a) Overall grid (the area of interest in the red box is refined), (b) area of interest, and (c) details of the vertical grid. The white circle denotes the rotational grid region for different simulation cases.

3. RESULTS

3.1. Evaluation of the CFD simulations

Table 1 shows the mean relative error (MRE) and the root-mean-square error (RMSE) values of the CFD-simulated wind speed and wind direction at the locations of the five observation towers. The field measurement data used for validation consist of 10-minute averages recorded from 30 June 2002 to 31 August 2003. The steady-state RANS solutions, representing time-averaged flow fields, were driven by inlet boundary conditions derived from the ERA5 reanalysis dataset with a temporal resolution of one hour and a spatial resolution of 0.25° × 0.25°. The simulation results are thus validated against the observational 10-minute mean values. As shown in Table 1, the RMSE of the wind speed ranges from 0.19 m/s to 0.56 m/s, with the MRE distributed between 4.13% and 14.62%. The mean values of RMSE for wind speed and wind direction are 0.40 m/s and 16.31°, respectively, and the mean value of MRE for wind speed is 8.22%. The above error values indicate that CFD can effectively simulate the near-surface wind fields of Nan'ao Island, with better performance for the wind speed than the wind direction.

Table 1. Errors of the CFD-simulated wind speed and wind direction at the locations of the five observation towers. The unit of the MRE is %, and the units of the RMSE values for the wind speed and wind direction are m/s and °.

Wind tower	10 m wind speed		20 m wind speed		30 m wind speed		40 m wind speed		50 m wind speed		10~50 m wind speed		50 m wind direction
	MRE	RMSE	MRE	RMSE	MRE	RMSE	MRE	RMSE	MRE	RMSE	MRE	RMSE	RMSE
1001	8.84	0.44	10.59	0.48	10.35	0.47	10.25	0.48	9.48	0.46	9.90	0.47	19.57
1002	11.12	0.45	/	/	/	/	9.33	0.45	10.18	0.48	6.13	0.46	19.6
1003	4.31	0.19	5.02	0.24	4.84	0.24	4.13	0.25	4.16	0.22	4.49	0.23	11.54
1004	13.21	0.52	14.62	0.56	12.34	0.46	14.83	0.51	12.05	0.48	13.41	0.51	18.65
1007	6.84	0.33	6.88	0.4	7.54	0.34	7.55	0.36	6.98	0.34	7.16	0.35	12.2
Mean value	8.86	0.39	7.42	0.42	7.01	0.38	9.22	0.41	8.57	0.40	**8.22**	**0.40**	**16.31**

3.2. Effects of the slope angle on the wind speed ratios

In this study, two parameters, the slope angle and the horizontal slope length, were selected to investigate the impact of local topography on the near-surface wind characteristics (wind speed ratio) over actual hilly terrain. Figure 3 shows a diagram of the calculation of the slope angle (α) and horizontal slope length (L). As shown in Figure 3, if the local wind blows from west to east, the slope angle of the grid point E can be calculated as

$$\alpha = \arctan\left(\frac{H - H_0}{L}\right), \tag{1}$$

where H and H_0 are the altitudes of points E and E_0, respectively, and L is the horizontal length between points E and E_0 and is defined as the "horizontal slope length" in this study, where E_0 is a point located upstream of point E at a horizontal distance of L. As shown in Equation (1), α is positive on the windward slope and negative on the leeward slope.

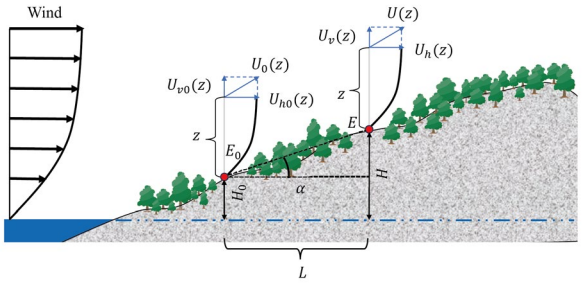

Figure 3. Diagram of the calculation of the slope angle (α) and horizontal slope length (L). $U(z)$, $U_h(z)$, and $U_v(z)$ are the total, horizontal, and vertical wind speeds, respectively, at point E at a height of z, and $U_0(z)$, $U_{h0}(z)$, and $U_{v0}(z)$ are the total, horizontal, and vertical wind speeds, respectively, at point E_0 at a height of z. E_0 is a point located upstream of point E at a horizontal distance of L.

The total wind speed ratios (S) is larger than 1.0 and increase with increasing slope angle when $\alpha < 32.5°$ under the uphill condition. Conversely, under the downhill condition, S is less than 1.0 and decrease with increasing slope angle. As for the wind field variations with height, the wind speed acceleration and deceleration are more pronounced near the surface than in the upper levels. In addition, when the slope angle is approximately 30°, the maximum acceleration and deceleration

of the 10-m wind speed between two neighboring points with a horizontal distance of 100 m can reach 45% under the uphill condition and 33% under the downhill condition.

3.3. Effects of the horizontal slope length on the wind speed ratios

Figure 4 shows the variation in the wind speed ratios with the slope angle at different horizontal slope lengths under the uphill and downhill conditions. As shown in Figure 4(a), S initially increases but then decrease with increasing L under the uphill condition. With increasing α, S first increases but then decrease after reaching a critical slope angle. Notably, the values of the critical slope angle generally decrease with increasing L. For example, the critical slope angle is approximately 27° when L is 100 m, while the critical slope angle is only 15° when L increases to 800 m. For downhill slopes, critical slope angles also exist for S (Figure 4(b)). Note that, when L is equal to or larger than 200 m, the wind speed ratio at 10 m exceeds 1.0, which indicates that acceleration occurs when descending over a gentle slope ($|\alpha| < \sim 6°$). The acceleration effect of a gentle slope can surpass 15% when L is 800 m. Provided that the slope angle is small enough to avoid airflow separation on the lee slope, the downhill terrain can still induce a significant wind field acceleration.

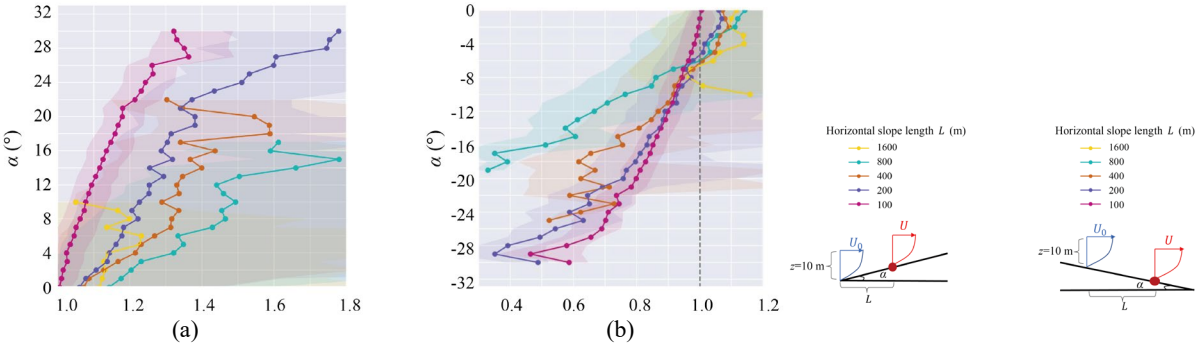

Figure 4. Variations in the total wind speed ratios (S) with slope angle (α) for different horizontal slope lengths (L) under the (a) uphill and (b) downhill conditions.

4. CONCLUSIONS

This study numerically investigated the influence of local topographic relief on the near-surface wind field over Nan'ao Island, China, using CFD simulations based on the RANS equations and the k–ε turbulence model for 16 wind directions under neutral atmospheric conditions. A novel evaluation method was proposed to validate the performance of the simulated wind field with ERA-5 reanalysis data and field measurements at five observation towers. The mean values of RMSE for wind speed and wind direction are 0.40 m/s and 16.31° respectively, indicating that CFD can effectively simulate the near-surface wind fields of Nan'ao Island.

The results reveal that terrain-induced wind speed acceleration ($S > 0$) and deceleration ($S < 0$) are most pronounced close to the surface. A critical slope angle was observed, where the horizontal wind speed ratio peaks under both uphill and downhill conditions. Furthermore, the vertical wind speed ratio increases with slope angle, whereas gentle downhill slopes ($|\alpha| < \sim 6°$) exhibit an unexpected wind acceleration effect. Comparisons with current load codes show that while simulations align well with standards like the Canadian and American codes for gentle slopes, significant discrepancies arise for steep slopes, where the topographic influence extends vertically

beyond code considerations. This underscores the necessity to optimize existing codes for steep uphill and gentle downhill terrains. The findings of this study enrich the understanding of the near-surface wind characteristics over natural hilly terrain and offer an effective method for evaluating the simulated wind field with ERA-5 reanalysis data and field measurements. Notably, this study was based on a case study of the wind field over a hilly island in neutral atmospheric conditions. Future work will consider thermal effects on the wind characteristics and expand the research sample to include a greater variety of terrain features, thereby enhancing the universality of the research findings.

ACKNOWLEDGEMENTS

This work was supported by the National Natural Science Foundation of China (No. 42275099).

REFERENCES

Blocken, B., van der Hout, A., Dekker, J., & Weiler, O. 2015. CFD simulation of wind flow over natural complex terrain: Case study with validation by field measurements for Ria de Ferrol, Galicia, Spain. *Journal of Wind Engineering and Industrial Aerodynamics*, *147*, 43-57. https://doi.org/10.1016/j.jweia.2015.09.007

Jubayer, C., & Hangan, H. 2018. A hybrid approach for evaluating wind flow over a complex terrain. *Journal of Wind Engineering and Industrial Aerodynamics*, *175*. https://doi.org/10.1016/j.jweia.2018.01.037

Moreira, G. A. A., dos Santos, A. A. C., do Nascimento, C. A. M., & Valle, R. M. 2012. Numerical Study of the Neutral Atmospheric Boundary Layer Over Complex Terrain. *Boundary-Layer Meteorology*, *143*(2), 393-407.